Neutrosophic Sets and Systems, Vol. 100, 2026
University of New Mexico

A Linguistic Neutrosophic TOPSIS Framework for Sustainable Biomass Composite Selection

KATHIRVEL Ayyaswamy[1], RAJENDRA THILAHAR Chelladurai[2], GOBINATH Vellapalayam Manoharan[3],*

[1] - Department of Computer Science, Saveetha Engineering College, Chennai, India. Email id: ayyakathir@gmail.com
[2] - Department of Artificial Intelligence and Data Sciences, Saveetha Engineering College, Chennai, India. Email id: thilahar74@gmail.com
[3,*] - Department of Robotics and AI, Chettinad Institute of Technology, Chettinad Academy of Research and Education, Chennai, Tamilnadu 603 103, India. Email id: vmgobinath@gmail.com

[*]- Corresponding Author: vmgobinath@gmail.com

Abstract

The valorization of agricultural waste biomass as functional filler in FDM 3D printing composites represents a tangible contribution towards sustainable additive manufacturing and circular economy synergism. Choosing the right composite for FDM is difficult because there are a number of technical, economic and environmental criteria which conflict. Further, experts do not have complete certainty about any of the criteria. The indeterminacy level that characterises experts' judgement on emerging and only partially characterised materials cannot be independently quantified by classical fuzzy sets and intuitionistic fuzzy sets. The present research proposes a Linguistic Neutrosophic TOPSIS (LN-TOPSIS) technique to assess and rank five alternatives of agricultural waste biomass composite materials sourced from Tamil Nadu like Sugarcane Bagasse/PLA (A1), Rice Husk Silica/ABS (A2), Coir Fibre/PHA (A3), Bamboo Particle/Nylon (A4) and Groundnut Shell Powder/PETG (A5). The criteria entail six ones with technical, environmental and economic dimensions. This includes Mechanical Performance (C1) index, Printability (C2), Sustainability (C3), Raw material cost (C4), Regional availability (C5) and Surface quality (C6). Criterion weights originating from the Best-Worst Method (BWM) are obtained with a consistency ratio of 0.027. Expert evaluations are carried out according to a two-round Delphi protocol and the Linguistic Neutrosophic Weighted Averaging (LNWA) operator aggregates the panel judgements. Every language assessment is tethered to published quantitative material property data to ensure transparency and reproducibility. According to the analysis, Sugarcane Bagasse/PLA (A1) is the most preferred alternative (CC=0.861), followed by Bamboo Particle/Nylon (A4, CC=0.744) and Rice Husk Silica/ABS (A2, CC=0.518). Across all 36 systematic weight-perturbation scenarios, the ranking remains invariant, and in a Monte Carlo simulation using 1000 Dirichlet-sampled weight vectors, A1 ranked first in 96.7 % of the runs. The Spearman rank correlations between five existing MCDM methods are between 0.90 and 1.00. It is as per literature available to us, this is one of the earliest applications of linguistic neutrosophic MCDM to agriculture waste biomass composite for FDM 3D printing.

Keywords: linguistic neutrosophic numbers, TOPSIS, multi-criteria decision-making, FDM 3D printing, biomass composites.

1. Introduction

Additive manufacturing, and Fused Deposition Modelling (FDM) in particular, has evolved from a rapid prototyping to a production technology in sectors such as aerospace, automotive, biomedical and education (Balasubramanian et al., 2024) At the same time, the desire to restructure the industrial ecosystem towards a circular economy has increased the interest in substituting petroleum-based polymer filament with biodegradable and waste-based biocomposites.

India produces hundreds of millions of tonnes of crop residues a year. Tamil Nadu, one of India's largest producers of sugarcane, rice, coconut, groundnut and bamboo, contributes a huge amount. Using these agro-waste streams as functional fillers in FDM-grade polymer composites helps in relieving the burden at disposal, renders cost-effectiveness in raw materials, and brings biodegradability in printed parts (Liu et al., 2019). Despite a growing literature on individual biomass–polymer composites for FDM, a systematic multi-criteria comparative evaluation anchored to Tamil Nadu-sourced materials within a neutrosophic decision framework remains, on the basis of the literature reviewed here, largely unreported.

Material selection for FDM is a genuinely conflicting decision problem. Candidate materials exhibit incompatible performance profiles: the most sustainable option may print poorly, while a mechanically superior composite may carry an unacceptable cost or environmental burden. Classical scoring methods oversimplify this situation by requiring crisp numerical inputs, which are inappropriate for expert evaluations of novel or incompletely characterised materials.

Smarandache (1998) proposed neutrosophic set theory as a generalization of fuzzy sets (Zadeh, 1965) and intuitionistic fuzzy sets (Atanassov, 1986) which overcomes their limitation through an independent indeterminacy membership function. Fang and Ye (2017) embed linguistic variables within the neutrosophic framework to obtain Linguistic Neutrosophic Numbers (LNNs), which express both the linguistic label an expert proposes and the reliability associated with that label. Nagarajan et al. (2023) validated neutrosophic MCDM for 3D printer selection, providing a directly analogous methodological precedent for the present work.

The principal contributions of this study are: (i) an LN-TOPSIS framework that reformulates classical TOPSIS entirely within the LNN space, including an LNN complement operator for cost-type criterion normalisation; (ii) criterion weights derived by the Best-Worst Method under an explicit consistency check, eliminating arbitrary weight assignment; (iii) expert linguistic assessments anchored to published quantitative material property data; (iv) a structured two-round Delphi elicitation protocol with a reported concordance statistic; (v) a two-tier sensitivity analysis combining 36 systematic weight perturbations with a 1000-run Monte Carlo simulation; and (vi) comparative validation against five competing MCDM methods computed from independent inputs. The remainder of the paper is organised as follows. Section 2 reviews the relevant literature. Section 3 presents the mathematical preliminaries. Section 4 develops the proposed methodology. Section 5 describes the case study, and Section 6 reports the numerical results. Sections 7 and 8 present the sensitivity and comparative analyses. Section 9 discusses the findings, and Section 10 concludes.

2. Literature Review

2.1 Biomass Composites for FDM 3D Printing

As Liu et al. (2019) showed, the tensile strength of sugarcane bagasse cellulose fibres was achieved in a PLA matrix which still retained FDM printability at loadings of up to 15 wt% and had a tensile strength of 38–52 MPa depending on print orientation. Paternina Reyes et al (2024) synthesized rice husk/PLA composite filaments which have better stiffness than neat PLA. The authors reported surface roughness drawbacks at higher filler loadings.

The bamboo fibre composites for additive manufacturing were reviewed by Balasubramanian et al. (2024). The tensile strengths (45–65 MPa) of bamboo/nylon systems and good dimensional accuracy of the FDM-printed specimens were also reported. Durfina et al. (2025) examine PHA blend application as material for FDM. They find promising elongation at break as well as very good biocompatibility. High odds of nozzle clogging (over 10 wt% coir fibre loading). Guo et al. (2018) includes property comparisons for lignocellulosic fillers who examined toughening agents in wood flour/PLA composites.

The recent reports find that while the material class is gaining momentum, it is not without challenges. As indicated by Adjei-Yeboah and Jahan (2026), survey results on natural fibre reinforced polymer composites pointed out the common hindrances to printability were hydrophilicity of the fibre, thermal degradation during extrusion and weak interfacial bonding. On the other hand, Ahmad and others (2023) researched filament manufacture and investigation with specific emphasis on natural fibre feedstocks. Trivedi et al. provide information about the property ranges achievable through bast-fibre PLA systems (2023), while Zhou et al. put these developments in the full additive manufacturing picture (2024) and Sanivada et al. (2020).

Two findings from this literature bear directly on the criteria adopted here. First, filler loading trades tensile strength against stiffness and impact resistance: Somsuk et al. (2025), comparing rice husk and rice straw in PLA under identical conditions, observed declining tensile strength at higher loadings alongside improved flexural modulus and impact resistance, with finer particle size and alkali treatment moderating the loss. Mazzanti et al. (2019b) attribute this pattern to fibre morphology governing stress transfer. Second, particulate shell fillers behave differently from fibrous ones: Salmah et al. (2013) and Karagöz (2024) report that coconut and walnut shell powders raise stiffness and hardness while contributing little to tensile strength, which is the property profile expected of the groundnut shell system evaluated here as A5. Paulo et al. (2023) and Hassan and Dahy (2025) provide contrasting data for continuous and aligned fibre architectures, which lie outside the short-fibre regime considered in this study.

Safaei et al. (2024) reported that agricultural shell powders offer hardness improvements in polymer matrices comparable to those of other particulate lignocellulosic fillers, but groundnut shell powder remains unexplored as a dedicated FDM filler. This absence of published FDM-specific data for GSP/PETG constitutes an explicit knowledge gap and motivates the inclusion of A5 as an alternative whose evaluation necessarily carries elevated indeterminacy.

2.2 Neutrosophic and Linguistic MCDM Methods

Biswas et al. (2016) first adapted TOPSIS to the single-valued neutrosophic environment and demonstrated improved discriminative capability over fuzzy TOPSIS for problems with incomplete information. Ye (2015) proposed an extended TOPSIS method for single-valued neutrosophic linguistic numbers in group decision-making. Fang and Ye (2017) formally introduced LNNs together with the weighted averaging operator adopted here, and Ye (2017, 2019) subsequently developed Bonferroni mean and Einstein operators for the same setting.

Parallel work has refined the aggregation and ranking machinery on which such methods depend. Ye (2016) developed weighted arithmetic and geometric averaging operators for neutrosophic linguistic numbers and applied them to manufacturing alternative selection, establishing the operator family the present study draws on. Wang (2024) demonstrated that the choice of score function materially changes single-valued neutrosophic rankings and proposed a standard-coefficient formulation, which motivates the explicit justification of the score function adopted in Section 3.4 rather than treating it as an arbitrary convention.

Nagarajan et al. (2023) applied the neutrosophic MCDM approach to the selection of 3D printer using three methods N-TOPSIS , N-WASPAS and N-MOORA and consistency of , N-TOPSIS , N-WASPAS and N-MOORA was established. Nagarajan et al. (2023) used TODIM under single valued neutrosophic environment to investigate the barriers to Industry 5.0 adoption. Broumi et al. (2020) algorithms for Interval-valued Neutrosophic Network Analysis. These studies establish the methodological lineage of the present work.

Research gap. Notwithstanding the growth of both literatures, no study integrates them for Tamil Nadu agricultural waste biomass composite selection in FDM 3D printing with transparent weight derivation, structured Delphi elicitation and multi-method comparative validation. The present study addresses this gap.

3. Mathematical Preliminaries

3.1 Neutrosophic Sets and Single Valued Neutrosophic Sets

Definition 1 (Neutrosophic set, Smarandache, 1998). Let X be a universe of discourse. A neutrosophic set A in X is characterised by a truth membership function $T_A(x)$, an indeterminacy membership function $I_A(x)$ and a falsity membership function $F_A(x)$, each mapping X into the non-standard unit interval $]^-0, 1^+[$, subject to $0 \leq T_A(x) + I_A(x) + F_A(x) \leq 3$.

Definition 2 (Single valued neutrosophic set, Wang et al., 2010). A single valued neutrosophic set restricts T, I and F to the standard interval [0, 1] with $0 \leq T + I + F \leq 3$. A single valued neutrosophic number is written $\tilde{n} = (T, I, F)$.

3.2 Linguistic Term Set

Definition 3 (Linguistic term set). An ordered seven-point set $S = \{s_0, s_1, \ldots, s_6\}$ is adopted, consistent with the human capacity for reliable linguistic discrimination (Miller, 1956) and widely used in neutrosophic MCDM (Fang & Ye, 2017, Nagarajan et al., 2023). A higher subscript denotes a more favourable evaluation. The associated neutrosophic triplets are given in Table 1.

Table 1 *Seven-point linguistic scale with associated neutrosophic membership values*

Linguistic term	Symbol	Index	Truth (T)	Indeterminacy (I)	Falsity (F)
Very High / Very Good	VH / VG	s_6	0.90	0.10	0.10
High / Good	H / G	s_5	0.70	0.20	0.20
Medium High / Fairly Good	MH / FG	s_4	0.60	0.30	0.30
Medium	M	s_3	0.50	0.50	0.50
Medium Low / Fairly Poor	ML / FP	s_2	0.40	0.55	0.50
Low / Poor	L / P	s_1	0.20	0.70	0.70
Very Low / Very Poor	VL / VP	s_0	0.10	0.90	0.90

Note. *Triplets follow Fang and Ye (2017). The scale is symmetric about s_3 in the linguistic index and monotone in T, with I and F increasing as the evaluation becomes less favourable.*

3.3 Linguistic Neutrosophic Numbers

Definition 4 (Linguistic neutrosophic number, Fang & Ye, 2017). An LNN is the pair $\tilde{L} = \langle s_\alpha, (T, I, F)\rangle$ with $s_\alpha \in S$, $\alpha \in \{0, \ldots, t\}$ and $T, I, F \in [0, 1]$ satisfying $0 \leq T + I + F \leq 3$, where $t = 6$ is the upper index of the linguistic scale. An LNN therefore encodes simultaneously what the expert asserts (the linguistic label) and how reliable that assertion is (the neutrosophic triplet).

Let $\tilde{L}_1 = \langle s_\alpha, (T_1, I_1, F_1)\rangle$ and $\tilde{L}_2 = \langle s_\beta, (T_2, I_2, F_2)\rangle$ be two LNNs and let $\lambda > 0$. The basic operations are:

$$\tilde{L}_1 \oplus \tilde{L}_2 = \langle s_{\alpha+\beta-\alpha\beta/t}, (T_1+T_2-T_1T_2, I_1I_2, F_1F_2)\rangle \quad (1)$$

$$\tilde{L}_1 \otimes \tilde{L}_2 = \langle s_{\alpha\beta/t}, (T_1T_2, I_1+I_2-I_1I_2, F_1+F_2-F_1F_2)\rangle \quad (2)$$

$$\lambda\tilde{L}_1 = \langle s_{t[1-(1-\alpha/t)^\lambda]}, (1-(1-T_1)^\lambda, I_1^\lambda, F_1^\lambda)\rangle \quad (3)$$

3.4 Score and Accuracy Functions

The score function serves as the primary ranking criterion. Its quadratic form captures the linguistic magnitude α/t and the neutrosophic reliability simultaneously, so that high indeterminacy depresses the score even when truth membership is large. The accuracy function breaks ties when two score values coincide.

Definition 5 (Score function; Fang & Ye, 2017). For an LNN $\tilde{L} = \langle s_\alpha, (T, I, F)\rangle$,

$$S(\tilde{L}) = (1/3t)(\alpha/t + T - I - F + 2)(\alpha/t + T - I/2 - F/2 + 1), \quad S(\tilde{L}) \in [0, 4/t] \quad (4)$$

Definition 6 (Accuracy function). For the same LNN,

$$H(\tilde{L}) = (1/2t)(\alpha/t + T - F + 1), \quad H(\tilde{L}) \in [0, 3/(2t)] \quad (5)$$

The attainable range of these functions follows from their algebraic form rather than from convention. Substituting the maximal LNN $\langle s_t,(1,0,0)\rangle$ into Eq. (4) gives $S = 12/(3t) = 4/t$, and the minimal LNN $\langle s_0,(0,1,1)\rangle$ gives $S = 0$, with $t = 6$ the score therefore maps onto [0, 2/3] rather than onto the full unit interval. The accuracy function maps onto [0, 3/(2t)] = [0, 1/4] by the same argument. Because both functions are used only ordinally to identify ideal solutions and to break ties, the restricted range does not affect any ranking, a rescaling $S^* = (t/4)S$ would map onto [0, 1] if a normalised score were required for reporting.

Comparison law: if $S(\tilde{L}_1) > S(\tilde{L}_2)$ then $\tilde{L}_1 \succ \tilde{L}_2$; if the scores are equal, the LNN with the larger accuracy value is preferred.

3.5 The LNWA Aggregation Operator

Definition 7 (Linguistic neutrosophic weighted averaging operator; Fang & Ye, 2017). For LNNs $\tilde{L}_j = \langle s_{\alpha j}, (T_j, I_j, F_j)\rangle$, $j = 1, \ldots, n$, with weights $\omega_j \in [0,1]$ and $\sum\omega_j = 1$:

$$\mathrm{LNWA}(\tilde{L}_1, \ldots, \tilde{L}_n) = \langle s_{t[1-\prod(1-\alpha_j/t)^{\omega_j}]}, (1-\prod(1-T_j)^{\omega_j}, \prod I_j^{\omega_j}, \prod F_j^{\omega_j})\rangle \quad (6)$$

3.6 Distance Measure between LNNs

Definition 8 (Normalised Euclidean distance). For $\tilde{L}_1 = \langle s_{\alpha_1}, (T_1, I_1, F_1)\rangle$ and $\tilde{L}_2 = \langle s_{\alpha_2}, (T_2, I_2, F_2)\rangle$ (Biswas et al., 2016 Ye, 2015)

$$d(\tilde{L}_1, \tilde{L}_2) = \sqrt{\{ ¼ [(\alpha_1/t - \alpha_2/t)^2 + (T_1 - T_2)^2 + (I_1 - I_2)^2 + (F_1 - F_2)^2] \}} \quad (7)$$

The factor 1/4 weights the four LNN components equally and guarantees $d \in [0, 1]$. This measure satisfies non-negativity, symmetry, the identity of indiscernibles and the triangle inequality, and therefore constitutes a metric on the LNN space.

3.7 Theoretical Properties of the Framework

The operators introduced above are stated as definitions in the source literature but their properties are rarely verified for a particular parameterisation. The five propositions below establish the properties on which the proposed method depends. Each was additionally checked numerically over 10^4 randomly sampled LNN tuples; the verification code is included in the supplementary material.

Proposition 1 (The distance measure is a bounded metric). The function d of Eq. (7) is a metric on the LNN space $\Omega = [0,t] \times [0,1]^3$, and $d(\tilde{L}1, \tilde{L}2) \in [0,1]$ with both bounds attained.

Proof. Write $\varphi(\tilde{L}) = (\alpha/t, T, I, F) \in [0,1]^4$. Then $d(\tilde{L}1, \tilde{L}2) = ½\|\varphi(\tilde{L}1) - \varphi(\tilde{L}2)\|_2$, so d is the Euclidean metric on $[0,1]^4$ composed with the injective map φ and scaled by ½. Non-negativity and symmetry are immediate. Since φ is injective, $d(\tilde{L}1, \tilde{L}2) = 0$ forces $\varphi(\tilde{L}1) = \varphi(\tilde{L}2)$ and hence $\tilde{L}1 = \tilde{L}2$, giving the identity of indiscernibles. The triangle inequality is inherited from the Euclidean norm, positive scaling preserving it. For the bounds, each of the four coordinate differences lies in $[-1,1]$, so $\|\varphi(\tilde{L}1) - \varphi(\tilde{L}2)\|_2 \leq 2$ and $d \leq 1$, with equality at $\tilde{L}1 = \langle s_0,(0,0,0)\rangle$ and $\tilde{L}2 = \langle s_t,(1,1,1)\rangle$; the lower bound is attained whenever $\tilde{L}1 = \tilde{L}2$. ■

The scaling factor ¼ inside the radical, which is often presented as a normalisation convention, is therefore exactly what places d on the unit interval.

Proposition 2 (Strict monotonicity of the score function). On the interior of Ω, S is strictly increasing in α and in T, and strictly decreasing in I and in F. Its range is [0, 4/t], attained at DZ(0,1,1)⟩ and DZ(1,0,0) respectively.

Proof. Put $u = \alpha/t$ and write $S = (1/3t)\cdot A\cdot B$ with $A = u + T - I - F + 2$ and $B = u + T - I/2 - F/2 + 1$. On Ω we have $A \geq 0$, since its minimum over the box is attained at $(u,T,I,F) = (0,0,1,1)$ where $A = 0$, and likewise $B \geq 0$ with the same minimiser. Differentiating, $\partial S/\partial u = \partial S/\partial T = (1/3t)(A + B)$ and $\partial S/\partial I = -(1/3t)(B + A/2)$, $\partial S/\partial F = -(1/3t)(B + A/2)$. Since A and B vanish simultaneously only at the single corner $(0,0,1,1)$, we have $A + B > 0$ on the interior, so the first two partials are strictly positive and the last two strictly negative there. Evaluating at the extreme points gives $A = 4$, $B = 3$ and $S = 12/(3t) = 4/t$ at $DZ(1,0,0)$ and $A = B = 0$ with $S = 0$ at $DZ(0,1,1)$.

Proposition 2 is what licenses the interpretation placed on the score throughout: an alternative cannot improve its score by becoming less certain, because indeterminacy enters with a strictly negative derivative. It also supplies the corrected codomain used in Section 3.4.

Proposition 3 (LNWA is idempotent, bounded and monotone). For LNNs $\tilde{L}_1, \ldots, \tilde{L}_n$ and weights ω summing to one, (i) if $\tilde{L}_j = \tilde{L}$ for all j then LNWA = $\tilde{L}$ (ii) each component of LNWA lies between the smallest and largest corresponding component of its arguments (iii) LNWA is non decreasing in each truth component and non increasing in each indeterminacy and falsity component.

Proof. (i) With $\alpha_j = \alpha$ for all j, the linguistic component becomes $t[1 - \prod(1-\alpha/t)^{\omega_j}] = t[1 - (1-\alpha/t)^{\sum\omega_j}] = t[1 - (1-\alpha/t)] = \alpha$, and identically $1 - (1-T)^1 = T$, $I^1 = I$, $F^1 = F$. (ii) The maps $x \mapsto 1 - \prod(1-x_j)^{\omega_j}$ and $x \mapsto \prod x_j^{\omega_j}$ are weighted quasi-arithmetic means, each lying between the minimum and maximum of its arguments, applying this coordinatewise gives the claim. (iii) Each component is differentiable and monotone in the stated direction on (0,1), since $\partial/\partial T_k\ [1 - \prod(1-T_j)^{\omega_j}] = \omega_k(1-T_k)^{\omega_k-1}\prod_{j\neq k}(1-T_j)^{\omega_j} > 0$, and similarly for the multiplicative components.

Idempotency matters for the Delphi design: if the panel reaches full agreement on a cell, aggregation returns that shared judgement unchanged rather than distorting it.

Proposition 4 (The complement is an involution and reverses order on the linguistic scale). The operator $\neg$ of Eq. (8) satisfies $\neg\neg\tilde{L} = \tilde{L}$ for every LNN. Moreover, restricted to the seven-point scale S of Table 1, $\neg$ reverses the score order exactly: $S(\neg s_0) > S(\neg s_1) > \ldots > S(\neg s_6)$.

Proof. For the first claim, $\neg\tilde{L} = \langle s_{t-\alpha},(F, 1-I, T)\rangle$, so $\neg\neg\tilde{L} = \langle s_{t-(t-\alpha)},(T, 1-(1-I), F)\rangle = \langle s_\alpha,(T,I,F)\rangle$. For the second, the seven scale points are symmetric in the linguistic index and satisfy $F = T'$ and $I \approx 1 - I'$ for the reflected term, so applying $\neg$ maps each term onto the neutrosophic profile of its reflection; evaluating Eq. (4) at all seven complemented terms yields the strictly decreasing sequence 0.5756, 0.3848, 0.2242, 0.1667, 0.0728, 0.0297, 0.0033 for s_0 through s_6.

Remark. Order reversal is a property of the admissible domain, not of Ω in general. Over arbitrary tuples in $[0,t] \times [0,1]^3$ the map $\neg$ is not strictly order-reversing, because the reflection $I \mapsto 1 - I$ is independent of T and F there. This is not a defect for the present method, whose entries are LNWA aggregates of scale points: reversal was verified to hold for all 399 comparable pairs in the aggregated matrix of Table 10. It does, however, mean that $\neg$ should not be applied to LNNs constructed outside a symmetric linguistic scale without re-checking the property.

Proposition 5 (Bounds and attainment of the closeness coefficient). For every alternative, $CC_i \in [0,1]$. Furthermore $CC_i = 1$ if and only if A_i attains the positive ideal solution on every criterion carrying non zero weight, and $CC_i = 0$ if and only if it attains the negative ideal solution on every such criterion.

Proof. By Proposition 1 the separation measures are non-negative sums of non negatively weighted distances, so $d^+_i \geq 0$ and $d^-_i \geq 0$ and hence $CC_i = d^-_i/(d^+_i + d^-_i) \in [0,1]$ whenever the denominator is positive. $CC_i = 1$ requires $d^+_i = 0$, that is $\sum_j w_j\, d(\tilde{r}_{ij}, \tilde{r}^+_j) = 0$, as every term is non negative this forces $d(\tilde{r}_{ij}, \tilde{r}^+_j) = 0$ for each j with $w_j > 0$, and the identity of indiscernibles then gives $\tilde{r}_{ij} = \tilde{r}^+_j$. The argument for $CC_i = 0$ is symmetric. The denominator vanishes only in the degenerate case where the positive and negative ideal solutions coincide on every weighted criterion, that is when all alternatives are indistinguishable.

Because the ideal solutions are drawn from the observed alternatives rather than from an abstract reference point, both bounds are attained in practice only by an alternative that dominates or is dominated on every criterion; the interior values reported in Table 12 are therefore the expected outcome for a set of genuinely conflicting alternatives.

4. The Proposed LN-TOPSIS Framework

The concept of TOPSIS was first introduced by Hwang and Yoon in 1981. TOPSIS or Technique for Order of Preference by Similarity to an Ideal Solution, is a method that determines the ranking of alternatives in relation to a positive ideal solution and a negative ideal solution. The LN-TOPSIS method reshapes every computing step within the LNN space to make sure that no defuzzification or scalarisation happens before the closeness coefficient is computed. The present formulation is distinguished by two choices.

Cost-criterion normalisation. Rather than inverting numerical values, cost-type criteria are normalised by the LNN complement, which maps a favourable-in-cost evaluation onto its benefit-equivalent while correctly transposing the truth and falsity components and reflecting the indeterminacy:

$$\tilde{r}_{ij} = \neg \tilde{L}_{ij} = \langle s_{t-\alpha}, (F, 1-I, T)\rangle \ \text{(cost)}; \quad \tilde{r}_{ij} = \tilde{L}_{ij} \ \text{(benefit)} \tag{8}$$

Weighted separation measures. Criterion weights enter the separation measures rather than the decision matrix. Applying scalar multiplication (Eq. 3) to the matrix and then computing unweighted distances would apply the weights twice — once in compressing the LNN towards the origin and again implicitly through the resulting distances — and would also distort the linguistic index non-linearly. The present formulation follows Biswas et al. (2016) and Ye (2015):

$$d^+_i = \sum_{j=1}^{n} w_j \cdot d(\tilde{r}_{ij}, \tilde{r}^+_j) \tag{9}$$

$$d^-_i = \sum_{j=1}^{n} w_j \cdot d(\tilde{r}_{ij}, \tilde{r}^-_j) \tag{10}$$

$$CC_i = d^-_i \,/\, (d^+_i + d^-_i), \quad CC_i \in [0, 1] \tag{11}$$

Alternatives are ranked in descending order of CC_i. Algorithm 1 states the complete procedure, and Figure 1 presents the corresponding flowchart.

Algorithm 1 *LN-TOPSIS for biomass composite material selection*

```
Input:  Alternatives A = {A₁,…,Aₘ}; criteria C = {C₁,…,Cₙ}; decision makers DM = {DM₁,…,DMₖ};
        linguistic scale S; criterion types (benefit / cost)
Output: Ranked alternatives with closeness coefficients CCᵢ

for each DMₖ do                                   ▷ Delphi Rounds 1 and 2
    construct linguistic matrix D̃ᵏ = [L̃ᵏᵢⱼ]ₘₓₙ, each entry drawn from Table 1
end for
for each (i, j) do                                ▷ Step 2: panel aggregation
    L̃ᵢⱼ ← LNWA(L̃¹ᵢⱼ, …, L̃ᵏᵢⱼ) with ωₖ = 1/K                  (Eq. 6)
end for
for each (i, j) do                                ▷ Step 3: normalisation
```

```
    r̃ᵢⱼ ← ¬L̃ᵢⱼ if Cⱼ is a cost criterion, else L̃ᵢⱼ              (Eq. 8)
end for
identify best criterion Cᴮ and worst criterion Cᵂ     ▷ Step 4: BWM weights
elicit vectors Aᴮ (best-to-others) and Aᵂ (others-to-worst)
solve min ξ s.t. |wᴮ/wⱼ − aᴮⱼ| ≤ ξ, |wⱼ/wᵂ − aⱼᵂ| ≤ ξ, ∑wⱼ = 1, wⱼ ≥ 0
verify consistency ratio CR = ξ* / CI < 0.10
for each criterion Cⱼ do                             ▷ Step 5: ideal solutions
    r̃⁺ⱼ ← argmaxᵢ S(r̃ᵢⱼ);  r̃⁻ⱼ ← argminᵢ S(r̃ᵢⱼ)                (Eq. 4)
end for
for each alternative Aᵢ do                           ▷ Steps 6–7
    d⁺ᵢ ← ∑ⱼ wⱼ d(r̃ᵢⱼ, r̃⁺ⱼ);   d⁻ᵢ ← ∑ⱼ wⱼ d(r̃ᵢⱼ, r̃⁻ⱼ)          (Eqs. 9–10)
    CCᵢ ← d⁻ᵢ / (d⁺ᵢ + d⁻ᵢ)                                        (Eq. 11)
end for
return alternatives sorted by descending CCᵢ
```

4.1 Computational Complexity

Let m be the number of alternatives, n the number of criteria and K the number of decision makers. Step 2 evaluates the LNWA operator once per matrix cell over K arguments, giving O(Kmn) elementary operations; this dominates the ranking pipeline. Normalisation (Step 3), identification of the ideal solutions (Step 5) and the separation measures (Step 6) each require a single pass over the mn cells with constant work per cell, contributing O(mn). Weight derivation is independent of m: the bisection on ξ terminates in $O(\log(1/\varepsilon))$ iterations, each solving a linear programme in n variables with 4n constraints. The overall cost of one complete ranking is therefore $O(Kmn + \log(1/\varepsilon)\cdot LP(n))$, which for the present problem ($m = 5$, $n = 6$, $K = 3$) is negligible.

The sensitivity analyses dominate total runtime. Systematic perturbation re-runs the ranking 6n times, and the Monte Carlo simulation N times, giving $O(N\cdot mn)$ for the latter since weights change but the aggregated matrix does not and can be computed once and reused. With $N = 1000$ the complete analysis reported here executes in under two seconds on a standard desktop, so the framework scales comfortably to problem sizes well beyond the present case study.

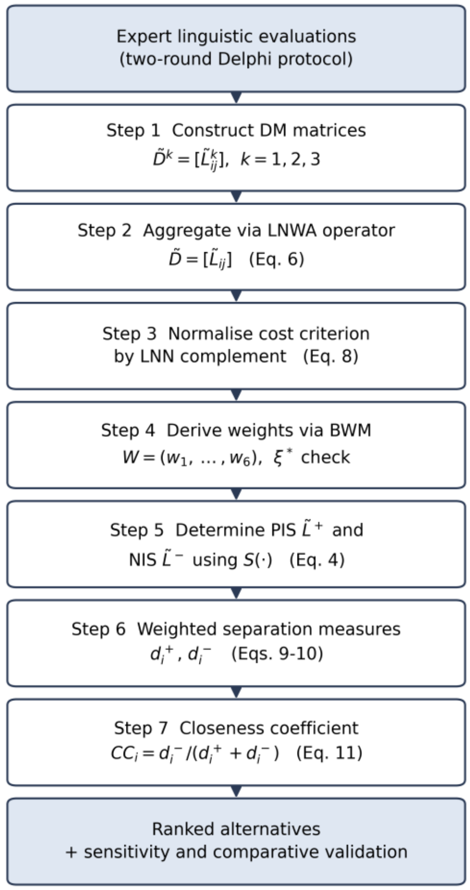

Figure 1 *Algorithmic flowchart of the proposed LN-TOPSIS framework.*

5. Case Study: Tamil Nadu Biomass Composite Selection

5.1 Alternatives

Five biomass-based composite filament alternatives, each derived from an agricultural waste stream available in Tamil Nadu, India, are considered (Table 2).

Table 2 *The five biomass composite alternatives and representative feedstock availability in Tamil Nadu*

Code	Composite	Biomass source	Polymer matrix	Representative sourcing districts
A1	Sugarcane Bagasse/PLA	SCB — sugar mills	PLA (biodegradable)	Erode, Villupuram, Cuddalore
A2	Rice Husk Silica/ABS	RHS — rice mills	ABS	Thanjavur, Tiruvarur
A3	Coir Fibre/PHA	CF — coconut processing	PHA (fully bio-based)	Nagercoil, Ramanathapuram
A4	Bamboo Particle/Nylon	BP — Western Ghats	Nylon PA12	Nilgiris, Coimbatore

Code	Composite	Biomass source	Polymer matrix	Representative sourcing districts
A5	Groundnut Shell Powder/PETG	GSP — groundnut mills	PETG	Vellore, Villupuram

5.2 Evaluation Criteria

Six criteria capture the technical, environmental and economic dimensions of the selection problem (Table 3). The criterion set was validated by literature review and by expert consensus during Round 1 of the Delphi process.

Table 3 *Evaluation criteria for biomass composite material selection*

Code	Criterion	Type	Dimension	Basis
C1	Mechanical Performance	Benefit	Technical	Tensile strength (MPa) and flexural modulus (GPa), anchored to Table 4
C2	Printability Index	Benefit	Technical	Filament feeding consistency, layer adhesion, warping, nozzle clogging risk at 10 wt% loading
C3	Sustainability Index	Benefit	Environmental	Biodegradability, carbon footprint and waste utilisation ratio from LCA literature
C4	Raw Material Cost	Cost	Economic	Estimated cost per kg of composite filament from Indian agri-waste market data
C5	Regional Availability	Benefit	Environmental	Tamil Nadu feedstock production volume (Mt/year)
C6	Surface Quality	Benefit	Technical	Surface roughness Ra (μm) of FDM-printed specimens; lower Ra is better

5.3 Literature-Anchored Quantitative Property Data

To anchor the linguistic assessments to objective evidence and to support reproducibility, Table 4 compiles quantitative property values for each alternative from the cited literature. Each decision maker consulted these values before assigning linguistic ratings. Where published values for a specific composite were unavailable — notably for A5 (GSP/PETG) — the corresponding expert ratings carry elevated indeterminacy, which propagates explicitly through the LNN arithmetic.

Table 4 *Literature-anchored quantitative material properties*

Alternative	Tensile strength (MPa)	Flexural modulus (GPa)	Surface roughness Ra (μm)	Biodegradability	Estimated cost (INR/kg)	Source
A1 SCB/PLA	38–52	2.8–3.5	8–14	High	350–500	Liu et al. (2019); Guo et al. (2018)
A2 RHS/ABS	35–48	2.4–3.1	12–20	Medium	400–600	Paternina Reyes et al. (2024)
A3 CF/PHA	28–40	1.8–2.6	14–22	Very High	450–650	Durfina et al. (2025)
A4 BP/Nylon	45–65	3.2–4.1	6–12	Medium	700–900	Balasubramanian et al. (2024)
A5 GSP/PETG a	25–35	1.5–2.2	18–28	Medium	300–450	Safaei et al. (2024)

Note. *a Values for A5 are estimated from analogous agricultural shell powder composites because no dedicated GSP/PETG FDM data have been published; expert ratings for A5 accordingly carry I ≥ 0.50. Biodegradability: Very High = >80% degradation in six months, High = 50–80%; Medium = 20–50% (adapted from Mazzanti et al., 2019a).*

5.4 Expert Panel and Delphi Elicitation

Three domain experts were selected against three criteria: at least ten years of relevant experience; an active publication record comprising no fewer than five Scopus-indexed papers on FDM, composite materials or sustainable manufacturing; and no financial relationship with any manufacturer of the assessed materials. All experts provided written informed consent and a conflict-of-interest declaration before participating. Panel profiles appear in Table 5.

Table 5 *Expert panel profiles*

Expert	Specialisation	Experience (years)	Institution type	Scopus publications	COI
DM1	Materials engineering and FDM composites	15	Engineering college, Tamil Nadu	18+	None declared
DM2	Additive manufacturing and process engineering	12	Research institute, India	12+	None declared
DM3	Sustainable manufacturing and circular economy	10	Technical university, India	10+	None declared

The panel was deliberately small. The evaluation requires simultaneous command of FDM process behaviour, lignocellulosic composite characterisation and sustainability assessment, and the criterion set could not be reliably rated by a specialist in only one of these areas. Three experts satisfying all three selection criteria were available without compromising the conflict-of-interest requirement, and a structured two-round Delphi with a reported concordance statistic was adopted precisely because it extracts a defensible consensus from a small expert group rather than relying on numerical averaging over a large one. The consequences for precision are stated explicitly in Section 10.1, and expanding the panel is identified there as a priority for subsequent work.

Round 1. Each expert independently reviewed the quantitative property data (Table 4) and the criterion definitions (Table 3), then assigned linguistic evaluations to every alternative–criterion pair using the seven-point scale. Divergent ratings were defined as those separated by two or more scale points.

Round 2. Divergent ratings were circulated anonymously to the full panel with the accompanying justifications, and experts were invited to revise. Agreement on the finalised Round 2 matrices, measured by Kendall's coefficient of concordance across the 30 alternative–criterion cells, is $W = 0.959$ ($\chi^2(29) = 83.40$, $p < 0.001$), indicating strong consensus. The finalised matrices constitute Tables 6–8.

5.5 Criterion Weights by the Best-Worst Method

To avoid arbitrary weight assignment, criterion weights are derived using the Best-Worst Method (Rezaei, 2015), which requires fewer pairwise comparisons than AHP and generally yields more consistent weights. Mechanical Performance (C1) was identified by panel consensus as the best criterion and Regional Availability (C5) as the worst. The best-to-others and others-to-worst vectors were elicited on a 1–9 scale as $A^B = (1, 2, 4, 8, 9, 3)$ and $A^W = (9, 4, 2, 1, 1, 3)$, read against C1–C6 respectively. Solving the minimax programme by bisection on ξ combined with linear-programming feasibility testing yields $\xi^* = 0.140$. With $a^{BW} = 9$, the corresponding consistency index is 5.23, giving a consistency ratio CR = 0.027, comfortably below the 0.10 threshold. The resulting weights appear in Table 6 and Figure 3.

Table 6 *BWM comparison vectors, derived criterion weights and consistency check*

Criterion	C1 Mech. perf.	C2 Printability	C3 Sustainability	C4 Cost	C5 Availability	C6 Surface quality
Best-to-others (A^B)	1	2	4	8	9	3
Others-to-worst (A^W)	9	4	2	1	1	3
Weight w_j	**0.441**	**0.206**	**0.106**	**0.054**	**0.050**	**0.142**
Rank	1	2	4	5	6	3

Note. *$\xi^* = 0.140$, $CI(a^{BW} = 9) = 5.23$, $CR = 0.027 < 0.10$ (Rezaei, 2015). Mechanical Performance carries the largest weight because FDM components must satisfy minimum structural requirements before other attributes become decision relevant Surface Quality ranks third, reflecting its importance for the visible, tactile parts typical of STEM education kits and consumer prototyping.*

6. Numerical Results

6.1 Finalised Linguistic Decision Matrices

Tables 6–8 report the Round 2 linguistic evaluations of the three decision makers. Each entry is a linguistic term from Table 1, assigned with reference to the quantitative anchors in Table 4.

Table 7 *Finalised linguistic evaluation matrix of DM1 (Delphi Round 2)*

Alternative	C1	C2	C3	C4 (cost)	C5	C6
A1 – SCB/PLA	G	VG	G	VL	VH	G
A2 – RHS/ABS	G	M	M	L	H	M
A3 – CF/PHA	M	M	VG	L	H	M
A4 – BP/Nylon	VG	G	M	M	M	VG
A5 – GSP/PETG	M	L	G	VL	H	L

Table 8 *Finalised linguistic evaluation matrix of DM2 (Delphi Round 2)*

Alternative	C1	C2	C3	C4 (cost)	C5	C6
A1 – SCB/PLA	VG	G	G	VL	VH	G
A2 – RHS/ABS	G	MH	MH	L	H	MH
A3 – CF/PHA	MH	M	VG	L	H	ML
A4 – BP/Nylon	VG	G	M	MH	ML	VG
A5 – GSP/PETG	M	ML	G	VL	MH	ML

Table 9 *Finalised linguistic evaluation matrix of DM3 (Delphi Round 2)*

Alternative	C1	C2	C3	C4 (cost)	C5	C6
A1 – SCB/PLA	G	VG	MH	VL	VG	MH
A2 – RHS/ABS	MH	MH	M	ML	H	M
A3 – CF/PHA	M	ML	VG	L	G	ML
A4 – BP/Nylon	VG	MH	ML	M	M	G

Alternative	C1	C2	C3	C4 (cost)	C5	C6
A5 – GSP/PETG	ML	L	MH	VL	H	L

6.2 Aggregated and Normalised LNN Decision Matrix

Applying the LNWA operator (Eq. 6) with equal decision-maker weights $\omega_k = 1/3$ produces the aggregated matrix in Table 10. The indeterminacy components for A5 are markedly higher than for the other alternatives across most criteria — for instance ⟨ $s_{2.70}$, (0.469, 0.516, 0.500)⟩ under C1 — which is precisely the epistemic situation created by the absence of published GSP/PETG FDM data. Neither classical nor fuzzy TOPSIS can represent this distinction: both would record a low rating without recording that the rating is itself unreliable.

Table 10 *Aggregated linguistic neutrosophic decision matrix [$\tilde{L}_{ij}$]*

Alt.	C1	C2	C3	C4	C5	C6
A1	<s6.00,(0.79,0.15,0.15)>	<s6.00,(0.85,0.12,0.12)>	<s4.74,(0.67,0.22,0.22)>	<s0.00,(0.10,0.90,0.90)>	<s6.00,(0.90,0.10,0.10)>	<s4.74,(0.67,0.22,0.22)>
A2	<s4.74,(0.67,0.22,0.22)>	<s3.71,(0.56,0.35,0.35)>	<s3.38,(0.53,0.42,0.42)>	<s1.36,(0.27,0.64,0.62)>	<s5.00,(0.70,0.20,0.20)>	<s3.38,(0.53,0.42,0.42)>
A3	<s3.38,(0.53,0.42,0.42)>	<s2.70,(0.46,0.51,0.50)>	<s6.00,(0.90,0.10,0.10)>	<s1.00,(0.20,0.70,0.70)>	<s5.00,(0.70,0.20,0.20)>	<s2.37,(0.43,0.53,0.50)>
A4	<s6.00,(0.90,0.10,0.10)>	<s4.74,(0.67,0.22,0.22)>	<s2.70,(0.46,0.51,0.50)>	<s3.38,(0.53,0.42,0.42)>	<s2.70,(0.46,0.51,0.50)>	<s6.00,(0.85,0.12,0.12)>
A5	<s2.70,(0.46,0.51,0.50)>	<s1.36,(0.27,0.64,0.62)>	<s4.74,(0.67,0.22,0.22)>	<s0.00,(0.10,0.90,0.90)>	<s4.74,(0.67,0.22,0.22)>	<s1.36,(0.27,0.64,0.62)>

Note. *Entries are written ⟨ s_a, (T, I, F)⟩ . C4 is a cost criterion and is normalised by the LNN complement (Eq. 8) before the ideal solutions are determined; the normalised C4 column is ⟨ s6.00, (0.900, 0.100, 0.100)⟩ , ⟨ s4.64, (0.626, 0.354, 0.273)⟩ , ⟨ s5.00, (0.700, 0.300, 0.200)⟩ , ⟨ s2.62, (0.422, 0.578, 0.536)⟩ and ⟨ s6.00, (0.900, 0.100, 0.100)⟩ for A1–A5 respectively.*

6.3 Score Matrix, Ideal Solutions and Worked Example

Score values $S(\tilde{r}_{ij})$ computed from the normalised matrix by Eq. (4) are reported in Table 11, together with the PIS and NIS identified per criterion. Because the score function is strictly increasing in the linguistic index and in truth membership, and strictly decreasing in indeterminacy and falsity, the ideal solutions correspond to the most and least reliable-and-favourable evaluations rather than merely the extreme linguistic labels.

Worked example. For A1 under C1 the three experts assigned G, VG and G, giving triplets (5, 0.70, 0.20, 0.20), (6, 0.90, 0.10, 0.10) and (5, 0.70, 0.20, 0.20). With $\omega_k = 1/3$, Eq. (6) gives a linguistic index of 6[1 − ((1−5/6)(1−6/6)(1−5/6))^(1/3)]. Because one expert assigned the maximal term s_6, the corresponding factor vanishes and the aggregated index is exactly s6.00. The truth component is 1 − [(0.30)(0.10)(0.30)]^(1/3) = 0.792, while the indeterminacy and falsity components are [(0.20)(0.10)(0.20)]^(1/3) = 0.159, yielding $\tilde{L}11$ = ⟨ s6.00, (0.792, 0.159, 0.159)⟩ . Substituting into Eq. (4):

$$S(\tilde{L}11) = (1/18)(1.000 + 0.792 - 0.159 - 0.159 + 2)(1.000 + 0.792 - 0.0795 - 0.0795 + 1) = 0.508.$$

The PIS under C1 is A4’s evaluation ⟨ s6.00, (0.900, 0.100, 0.100)⟩ with score 0.576, so A1 sits close to but below the ideal on the most heavily weighted criterion. The weighted separation contribution of this cell is $w_1 \cdot d(\tilde{L}11, \tilde{r}^{+}_{1}) = 0.441 \times 0.068 = 0.030$.

Table 11 *Score values $S(\tilde{r}_{ij})$ of the normalised LNN matrix with ideal solutions*

Alternative	C1 (w = 0.441)	C2 (w = 0.206)	C3 (w = 0.106)	C4 (w = 0.054)	C5 (w = 0.050)	C6 (w = 0.142)
A1 – SCB/PLA	0.508	0.546	0.372	0.576	0.576	0.372
A2 – RHS/ABS	0.372	0.252	0.210	0.321	0.406	0.210
A3 – CF/PHA	0.210	0.149	0.576	0.385	0.406	0.131
A4 – BP/Nylon	0.576	0.372	0.149	0.126	0.149	0.546
A5 – GSP/PETG	0.149	0.059	0.372	0.576	0.372	0.059
PIS $\tilde{r}^{+}_{j}$	**0.576**	**0.546**	**0.576**	**0.576**	**0.576**	**0.546**
NIS $\tilde{r}^{-}_{j}$	**0.149**	**0.059**	**0.149**	**0.126**	**0.149**	**0.059**

Note. *C4 scores are computed on the complement-normalised entries, so a higher value denotes a lower raw material cost. A1 and A5 share the maximum C4 score because both were rated VL on raw cost by all three experts.*

6.4 Separation Measures and Final Ranking

Weighted separation measures and closeness coefficients follow from Eqs. (9)–(11); results are given in Table 12 and visualised in Figure 2. The final ranking is A1 ≻ A4 ≻ A2 ≻ A3 ≻ A5.

Table 12 *Separation measures, closeness coefficients and final ranking*

Alternative	d^{+}_{i}	d^{-}_{i}	CC_i	Rank
A1 – SCB/PLA	0.072	0.445	0.861	1 (best)
A2 – RHS/ABS	0.247	0.265	0.518	3
A3 – CF/PHA	0.332	0.178	0.349	4
A4 – BP/Nylon	0.130	0.378	0.744	2
A5 – GSP/PETG	0.439	0.070	0.138	5 (worst)

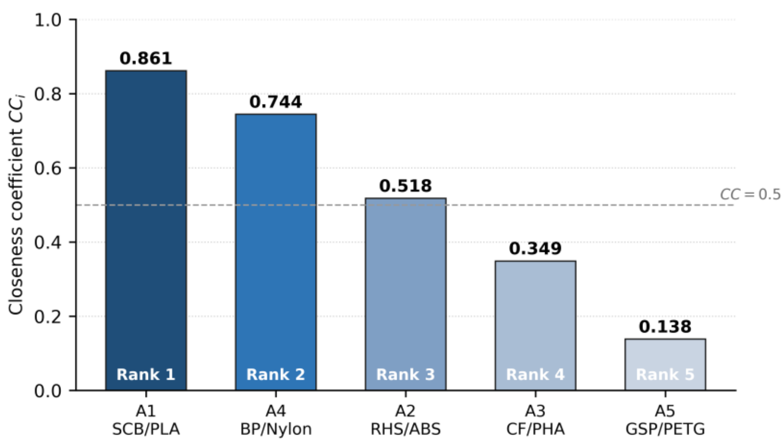

Figure 2 *Closeness coefficients CC_i and final ranking of the five alternatives.*

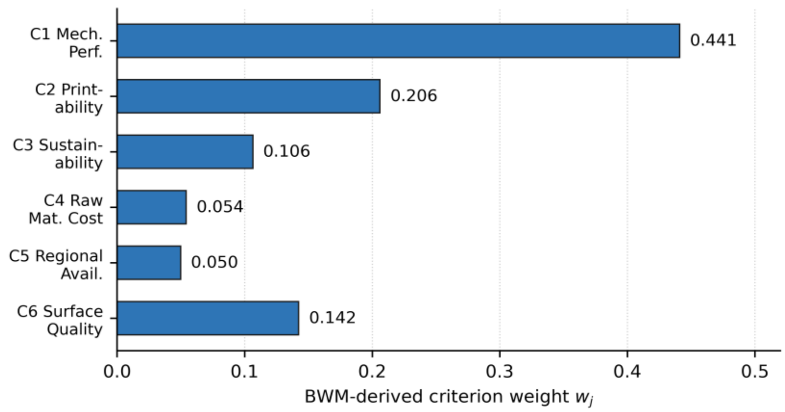

Figure 3 *BWM-derived criterion weights (ξ* = 0.140, CR = 0.027).*

7. Sensitivity Analysis

7.1 Systematic Weight Perturbation

Each criterion weight was perturbed by ±10%, ±20% and ±30% in turn, with the remaining weights rescaled proportionally so that the weight vector continued to sum to unity. This produces 36 distinct scenarios. The ranking A1 ≻ A4 ≻ A2 ≻ A3 ≻ A5 is preserved in all 36 cases, and no rank reversal occurs at any perturbation level for any criterion. Table 13 reports the closeness coefficients at the ±30% extremes, where the effect is largest; Figure 4 plots the full trajectories.

Table 13 *Closeness coefficients under ±30% weight perturbation of each criterion*

Perturbed criterion	Level	A1	A2	A3	A4	A5	Ranking preserved
C1	-30%	0.862	0.499	0.380	0.692	0.167	Yes
C1	+30%	0.860	0.537	0.316	0.800	0.108	Yes
C2	-30%	0.848	0.517	0.354	0.745	0.151	Yes
C2	+30%	0.874	0.518	0.343	0.744	0.126	Yes
C3	-30%	0.869	0.528	0.328	0.768	0.123	Yes
C3	+30%	0.853	0.508	0.369	0.720	0.153	Yes
C4	-30%	0.859	0.518	0.343	0.757	0.124	Yes
C4	+30%	0.863	0.518	0.354	0.732	0.152	Yes
C5	-30%	0.859	0.516	0.344	0.755	0.131	Yes
C5	+30%	0.863	0.520	0.353	0.734	0.145	Yes
C6	-30%	0.868	0.523	0.355	0.729	0.146	Yes
C6	+30%	0.854	0.513	0.342	0.759	0.130	Yes

Note. *All 36 scenarios (six criteria × six perturbation levels) preserve the baseline ranking; the ±30% extremes are shown because intermediate levels lie strictly between them.*

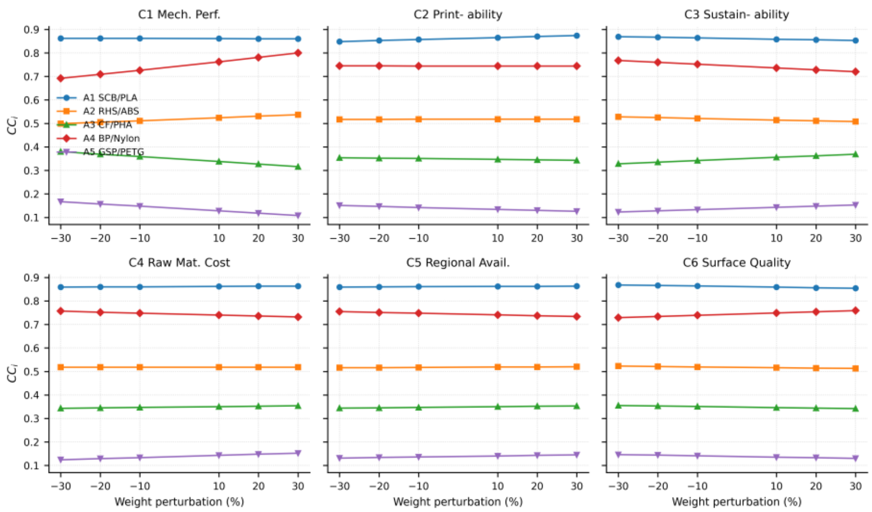

Figure 4 *Closeness-coefficient trajectories under systematic weight perturbation of each criterion.*

7.2 Monte Carlo Simulation

Systematic perturbation explores a neighbourhood of the elicited weight vector. To probe robustness across the entire weight simplex, 1000 weight vectors were drawn from a symmetric Dirichlet distribution with all concentration parameters equal to one, which is uniform over the simplex, and the full LN-TOPSIS procedure was executed for each draw (random seed 42). Table 14 reports the resulting rank frequency distribution and Figure 5 visualises it.

Table 14 *Monte Carlo rank frequency distribution (n = 1000 uniform Dirichlet weight vectors)*

Alternative	Rank 1 (%)	Rank 2 (%)	Rank 3 (%)	Rank 4 (%)	Rank 5 (%)	Mean rank	SD of CC_i
A1 – SCB/PLA	96.7	3.3	0.0	0.0	0.0	1.03	0.055
A2 – RHS/ABS	0.0	15.3	55.3	29.3	0.1	3.14	0.053
A3 – CF/PHA	1.1	32.6	18.8	47.4	0.1	3.13	0.107
A4 – BP/Nylon	2.2	44.5	11.0	9.7	32.6	3.26	0.177
A5 – GSP/PETG	0.0	4.3	14.9	13.6	67.2	4.44	0.148

The two poles of the ranking are highly stable: A1 occupies Rank 1 in 96.7% of draws with a mean rank of 1.03, and A5 occupies Rank 5 in 67.2% of draws. The intermediate positions are considerably less stable. A2, A3 and A4 have mean ranks of 3.14, 3.13 and 3.26 respectively — statistically indistinguishable — and A4 in particular ranges from Rank 1 in 2.2% of draws to Rank 5 in 32.6%. This dispersion is substantively informative rather than a defect of the method. A4 is the mechanically strongest alternative but the most expensive and least sustainable; under weight vectors that heavily favour cost or sustainability it falls to last place, while under mechanically dominated vectors it leads. The uniform Dirichlet prior samples such extreme vectors freely, whereas the elicited weights and the ±30% neighbourhood examined in Section 7.1 do not.

The appropriate reading is therefore twofold. The recommendation of A1 is robust both locally and globally. The ordering among A2, A3 and A4 is robust within the elicited weight neighbourhood but is contingent on the relative emphasis placed on mechanical performance, cost and sustainability, and should be revisited whenever an application context implies materially different priorities.

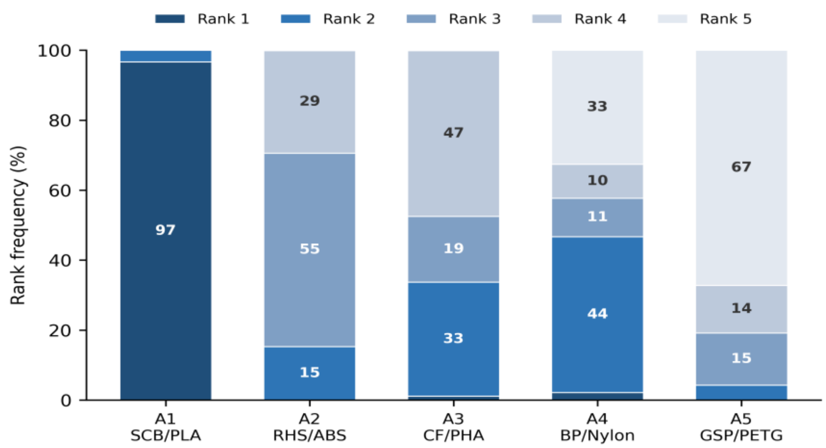

Figure 5 *Monte Carlo rank frequency distribution over 1000 uniform Dirichlet weight vectors.*

8. Comparative Study

The same decision problem was solved by five established MCDM methods. To avoid the circularity that would arise from feeding the neutrosophic score matrix into every comparator, each baseline is computed from inputs appropriate to it: classical TOPSIS operates on the quantitative property midpoints of Table 4; fuzzy TOPSIS operates on triangular fuzzy numbers derived directly from the same linguistic evaluations; and VIKOR ($v = 0.5$), WASPAS ($\lambda = 0.5$) and COPRAS operate on the defuzzified centroids of those triangular numbers. All methods use the BWM weights of Table 6. Results appear in Tables 15–16 and Figure 6.

Table 15 *Comparative rankings across six MCDM methods*

Alternative	LN-TOPSIS (proposed)	Classical TOPSIS	Fuzzy TOPSIS	VIKOR	WASPAS	COPRAS
A1 – SCB/PLA	1	2	1	1	1	1
A2 – RHS/ABS	3	3	3	3	3	3
A3 – CF/PHA	4	4	4	4	5	4
A4 – BP/Nylon	2	1	2	2	2	2
A5 – GSP/PETG	5	5	5	5	4	5

Table 16 *Spearman rank correlation with the LN-TOPSIS ranking*

Method	Spearman ρ	Divergence from LN-TOPSIS
Classical TOPSIS	0.90	A1/A4 order reversed
Fuzzy TOPSIS	1.00	None
VIKOR	1.00	None
WASPAS	0.90	A3/A5 order reversed
COPRAS	1.00	None

Three of the five comparators reproduce the LN-TOPSIS ranking exactly ($\rho = 1.00$) and the remaining two agree at $\rho = 0.90$, so all six methods identify A1 among the top two and none places A5 higher than fourth. The two divergences are informative. Classical TOPSIS, working from crisp property midpoints, promotes

A4 above A1 because it registers A4's superior tensile strength and surface finish without registering that the underlying expert judgements on A4's cost and sustainability are comparatively unfavourable and that its overall profile is narrower. WASPAS reverses A3 and A5 because its multiplicative component penalises A3's very weak printability score more aggressively than the additive distance measure of TOPSIS does.

Discriminative capability. The distinctive contribution of the neutrosophic representation is visible in the treatment of A5. Under fuzzy TOPSIS, A5's closeness coefficient is 0.160, which reflects only that experts rated it poorly. Under LN-TOPSIS it is 0.138, appreciably lower, because the indeterminacy components attached to A5's ratings ($I \geq 0.50$ across five of six criteria) enter the score function directly and depress it further. The framework therefore distinguishes an alternative that is confidently judged mediocre from one that is judged mediocre with low confidence — a distinction that is unavailable in the fuzzy setting and that matters materially when the decision concerns whether to commit experimental resources to an uncharacterised material.

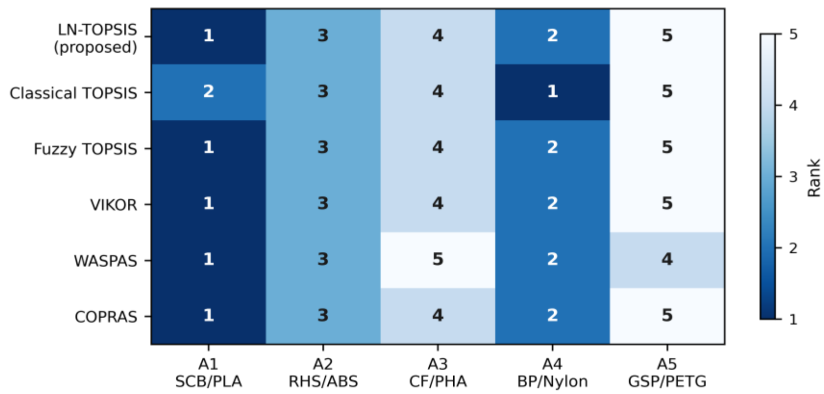

Figure 6 *Rank agreement across the six MCDM methods.*

9. Discussion

Sugarcane Bagasse/PLA emerges as the preferred alternative with CC = 0.861, a margin of 0.117 over the runner-up, and it holds Rank 1 in all 36 systematic perturbation scenarios and in 96.7% of Monte Carlo draws. Its advantage is one of balance rather than dominance: it attains the maximum score on three of six criteria (raw material cost, regional availability and printability) and the second-highest on mechanical performance, without falling to last place on any criterion. In the LNN representation its evaluations also carry consistently low indeterminacy, reflecting the comparatively mature published literature on bagasse-reinforced PLA. Practically, sugarcane bagasse is available in bulk from sugar mills in Erode, Villupuram and Cuddalore, and PLA is already the dominant FDM feedstock, so neither the filler supply chain nor the printing process requires reconfiguration.

Bamboo Particle/Nylon ranks second (CC = 0.744) on the strength of the highest mechanical performance and surface quality scores in the set. Its limitations are economic and environmental: it carries the highest estimated cost and the lowest score on regional availability, and nylon's non-biodegradability constrains its circularity credentials. The Monte Carlo results quantify this trade-off explicitly, with A4 appearing at both extremes of the ranking depending on the weight vector sampled. It is the appropriate recommendation for load-bearing applications where mechanical margin dominates cost.

Rice Husk Silica/ABS ranks third (CC = 0.518) with an unremarkable but consistent profile, while Coir Fibre/PHA ranks fourth (CC = 0.349) despite attaining the maximum sustainability score. The latter result illustrates why single-criterion optimisation misleads: A3's environmental credentials are offset by the weakest printability and surface quality scores in the set, and with sustainability weighted at 0.106 against the 0.789 commanded jointly by the three technical criteria, that trade is unfavourable under the elicited priorities. Where a decision context weights sustainability substantially higher, the sensitivity analysis indicates A3 becomes competitive.

Groundnut Shell Powder/PETG ranks last (CC = 0.138). This should be read as a statement about the current evidence base rather than about the material itself. A5 has the joint-lowest raw material cost and adequate regional availability, but no dedicated GSP/PETG FDM characterisation has been published, so every technical rating rests on analogy with other shell-powder composites. The neutrosophic framework records this as elevated indeterminacy rather than concealing it inside a point estimate, and the resulting low closeness coefficient is therefore best interpreted as identifying A5 as the alternative for which additional experimental characterisation would be most informative.

Methodologically, the framework contributes three elements beyond the existing linguistic neutrosophic TOPSIS literature. The LNN complement provides a principled normalisation for cost-type criteria that preserves the neutrosophic structure, whereas the common practice of inverting numerical values operates only on the linguistic index and leaves the reliability components untransformed. Deriving weights through BWM with an explicit consistency check removes the arbitrariness that attends direct weight assignment. Finally, the two-tier sensitivity design separates local robustness in the neighbourhood of the elicited weights from global robustness across the simplex, and reporting both prevents the overstatement of stability that a single analysis of either kind would invite.

10. Conclusions

This study developed a Linguistic Neutrosophic TOPSIS framework for selecting biomass-based composite materials for FDM 3D printing and applied it to five Tamil Nadu-sourced agricultural waste composites evaluated on six technical, environmental and economic criteria. Expert judgements were elicited through a two round Delphi protocol with strong final concordance ($W = 0.959$, $p < 0.001$), aggregated by the LNWA operator, and weighted by BWM derived coefficients with a consistency ratio of 0.027. Sugarcane Bagasse reinforced PLA is identified as the preferred alternative (CC = 0.861), ahead of Bamboo Particle reinforced Nylon (CC = 0.744). The ranking is invariant across all 36 systematic weight perturbation scenarios, A1 leads in 96.7% of 1000 Monte Carlo draws, and five independent MCDM comparators agree with the proposed ranking at $\rho \geq 0.90$.

10.1 Limitations

Four limitations qualify these findings. First, the evaluation rests on expert judgement anchored to published literature rather than on experimental characterisation of the five composites, and no specimens were fabricated or tested in this study; the results are therefore a structured evidence synthesis rather than an empirical comparison. Second, the panel comprises three experts, which is at the lower end of the acceptable range for Delphi studies and limits the precision of the concordance estimate. Third, criterion independence is assumed, whereas mechanical performance and surface quality are likely to be correlated through filler loading and particle morphology. Fourth, the property data underlying Table 4 are drawn from studies that differ in print parameters, specimen geometry and testing standard, so cross-study comparability is imperfect — and for A5 the data are estimated by analogy rather than measured.

10.2 Practical Implications

For manufacturers and filament producers in Tamil Nadu, sugarcane bagasse/PLA represents the most defensible entry point for agri-waste valorisation in FDM, combining an established feedstock supply, low cost and compatibility with existing PLA printing practice. For policy and circular economy programmes, the analysis identifies bagasse and rice husk streams as those where processing investment would yield the broadest applicability. For researchers, the framework is directly transferable to other biomass systems, other additive manufacturing processes such as SLA and SLS, and other regional agricultural waste contexts.

10.3 Future Work

Priorities for subsequent work follow from the limitations. Physical fabrication and characterisation of SCB/PLA and GSP/PETG filaments — tensile testing, scanning electron microscopy and thermal analysis — would allow the expert-based assessments to be validated against measurement, with A5 the highest-value target given its current indeterminacy. Extending the panel and applying neutrosophic DEMATEL would address the independence assumption by modelling criterion interdependency explicitly. Integrating life cycle assessment data would replace the composite sustainability index with quantified carbon footprint differentials, and coupling the framework to digital twin simulation of FDM process parameters would supply process-specific printability data in place of expert estimates.

Declarations

Compliance with Ethical Standards

The authors confirm that this manuscript is an original work that has not been published previously and is not under consideration for publication elsewhere, in whole or in part. All authors have contributed significantly to the research and preparation of this manuscript and have approved its final version for submission.

Funding

This research did not receive any specific grant from funding agencies in the public, commercial, or not-for-profit sectors.

Competing Interests

The authors declare that there are no competing interests, financial or non-financial, that could have influenced the work reported in this manuscript.

Ethics Approval and Consent to Participate

This article does not contain any studies with human participants or animals performed by the author. Informed consent was not required as this study does not involve human participants.

Data availability statement

The datasets generated and analysed during the current study are available from the corresponding author upon reasonable request.

References

Adjei-Yeboah, J., & Jahan, M. P. (2026). Additive manufacturing of natural fiber reinforced polymer composites: A review. Journal of Thermoplastic Composite Materials. https://doi.org/10.1177/08927057261415828

Ahmad, M. N., Ishak, M. R., Mohammad Taha, M., Mustapha, F., & Leman, Z. (2023). A review of natural fiber-based filaments for 3D printing: Filament fabrication and characterization. Materials, 16(11), 4052. https://doi.org/10.3390/ma16114052

Atanassov, K. T. (1986). Intuitionistic fuzzy sets. Fuzzy Sets and Systems, 20(1), 87–96. https://doi.org/10.1016/S0165-0114(86)80034-3

Balasubramanian, M., Saravanan, R., Sathish, T., Giri, J., Zairov, R., Hasnain, S. M. M., & Turmanov, R. (2024). Opportunities and challenges of bamboo fiber composites in additive manufacturing: A comprehensive review. AIP Advances, 14(9), 090702. https://doi.org/10.1063/5.0227267

Biswas, P., Pramanik, S., & Giri, B. C. (2016). TOPSIS method for multi-attribute group decision-making under single-valued neutrosophic environment. Neural Computing and Applications, 27(3), 727–737. https://doi.org/10.1007/s00521-015-1891-2

Broumi, S., Nagarajan, D., Lathamaheswari, M., Talea, M., Bakali, A., & Smarandache, F. (2020). Intelligent algorithm for trapezoidal interval valued neutrosophic network analysis. CAAI Transactions on Intelligence Technology, 5(2), 88–93. https://doi.org/10.1049/trit.2019.0086

Ďurfina, M., Babaei, N., Vanovčanová, Z., Feranc, J., Horváth, V., Vašková, I., Kruželák, J., Tomanová, K., & Plavec, R. (2025). Bio-based polyhydroxyalkanoate (PHA) blends for 3D printing: Rheological, mechanical, biocompatibility, and biodegradation properties. Polymers, 17(11), 1477. https://doi.org/10.3390/polym17111477

Fang, Z., & Ye, J. (2017). Multiple attribute group decision-making method based on linguistic neutrosophic numbers. Symmetry, 9(7), 111. https://doi.org/10.3390/sym9070111

Guo, R., Ren, Z., Bi, H., Song, Y., & Xu, M. (2018). Effect of toughening agents on the properties of poplar wood flour/poly(lactic acid) composites fabricated with fused deposition modeling. European Polymer Journal, 107, 34–45. https://doi.org/10.1016/j.eurpolymj.2018.07.035

Hassan, A., & Dahy, H. (2025). Continuous natural fiber-reinforced shape memory polymer biocomposites: Design and fabrication for sustainable self-folding architectural applications. Smart Materials and Structures, 34(1), 015051. https://doi.org/10.1088/1361-665X/ad9c06

Hwang, C. L., & Yoon, K. (1981). Multiple attribute decision making: Methods and applications. Springer. https://doi.org/10.1007/978-3-642-48318-9

Karagöz, İ. (2024). Production and characterization of sustainable biocompatible PLA/walnut shell composite materials. Polymer Bulletin, 81(13), 11517–11537. https://doi.org/10.1007/s00289-024-05247-4

Liu, H., He, H., Peng, X., Huang, B., & Li, J. (2019). Three-dimensional printing of poly(lactic acid) bio-based composites with sugarcane bagasse fiber: Effect of printing orientation on tensile performance. Polymers for Advanced Technologies, 30(4), 910–922. https://doi.org/10.1002/pat.4524

Mazzanti, V., Malagutti, L., & Mollica, F. (2019a). FDM 3D printing of polymers containing natural fillers: A review of their mechanical properties. Polymers, 11(7), 1094. https://doi.org/10.3390/polym11071094

Mazzanti, V., Pariante, R., Bonanno, A., Ruiz de Ballesteros, O., Mollica, F., & Filippone, G. (2019b). Reinforcing mechanisms of natural fibers in green composites: Role of fibers morphology in a PLA/hemp model system. Composites Science and Technology, 180, 51–59. https://doi.org/10.1016/j.compscitech.2019.05.015

Miller, G. A. (1956). The magical number seven, plus or minus two: Some limits on our capacity for processing information. Psychological Review, 63(2), 81–97. https://doi.org/10.1037/h0043158

Nagarajan, D., Gobinath, V. M., & Broumi, S. (2023). Multicriteria decision making on 3D printers for economic manufacturing using neutrosophic environment. Neutrosophic Sets and Systems, 57, 33–56. https://doi.org/10.5281/zenodo.8271321

Nagarajan, D., Kavikumar, J., Gobinath, V. M., & Broumi, S. (2023). Investigation of Industry 5.0 hurdles and their mitigation tactics in emerging economies by TODIM arithmetic and geometric aggregation operators in single value neutrosophic environment. Facta Universitatis, Series: Mechanical Engineering, 21(3), 405–432. https://doi.org/10.22190/FUME230616020D

Paternina Reyes, M. J., Unfried Silgado, J., Santa Marin, J. F., & Colorado Lopera, H. A. (2024). Rice husk with PLA: 3D filament making and additive manufacturing of samples for potential structural applications. Polymers, 16(2), 245. https://doi.org/10.3390/polym16020245

Paulo, A., Santos, J., da Rocha, J., Lima, R., & Ribeiro, J. (2023). Mechanical properties of PLA specimens obtained by additive manufacturing process reinforced with flax fibers. Journal of Composites Science, 7(1), 27. https://doi.org/10.3390/jcs7010027

Rezaei, J. (2015). Best-worst multi-criteria decision-making method. Omega, 53, 49–57. https://doi.org/10.1016/j.omega.2014.11.009

Safaei, B., Memarzadeh, A., Asmael, M., Sahmani, S., Zeeshan, Q., Jen, T.-C., & Qin, Z. (2024). Challenges and advancements in additive manufacturing of nylon and nylon composite materials. Journal of Materials Engineering and Performance. https://doi.org/10.1007/s11665-024-09368-9

Salmah, H., Koay, S. C., & Hakimah, O. (2013). Surface modification of coconut shell powder filled polylactic acid biocomposites. Journal of Thermoplastic Composite Materials, 26(6), 809–819. https://doi.org/10.1177/0892705711429981

Sanivada, U. K., Mármol, G., Brito, F. P., & Fangueiro, R. (2020). PLA composites reinforced with flax and jute fibers—A review of recent trends, processing parameters and mechanical properties. Polymers, 12(10), 2373. https://doi.org/10.3390/polym12102373

Smarandache, F. (1998). Neutrosophy: Neutrosophic probability, set, and logic. American Research Press.

Somsuk, N., Pramoonmak, S., Chongkolnee, B., Tipboonsri, P., & Memon, A. (2025). Enhancing mechanical properties of 3D-printed PLA composites reinforced with natural fibers: A comparative study. Journal of Composites Science, 9(4), 180. https://doi.org/10.3390/jcs9040180

Trivedi, A. K., Gupta, M. K., & Singh, H. (2023). PLA based biocomposites for sustainable products: A review. Advanced Industrial and Engineering Polymer Research, 6(4), 382–395. https://doi.org/10.1016/j.aiepr.2023.02.002

Wang, F. (2024). Novel score function and standard coefficient-based single-valued neutrosophic MCDM for live streaming sales. Information Sciences, 654, 119836. https://doi.org/10.1016/j.ins.2023.119836

Wang, H., Smarandache, F., Zhang, Y. Q., & Sunderraman, R. (2010). Single valued neutrosophic sets. Multispace and Multistructure, 4, 410–413.

Ye, J. (2015). An extended TOPSIS method for multiple attribute group decision making based on single valued neutrosophic linguistic numbers. Journal of Intelligent & Fuzzy Systems, 28(1), 247–255. https://doi.org/10.3233/IFS-141143

Ye, J. (2016). Aggregation operators of neutrosophic linguistic numbers for multiple attribute group decision making. SpringerPlus, 5, 1691. https://doi.org/10.1186/s40064-016-3247-5

Ye, J. (2017). Bonferroni mean operators of linguistic neutrosophic numbers and their multiple attribute group decision-making methods. Information, 8(3), 107. https://doi.org/10.3390/info8030107

Ye, J. (2019). Linguistic neutrosophic numbers Einstein operator and its application in decision making. Mathematics, 7(5), 389. https://doi.org/10.3390/math7050389

Zadeh, L. A. (1965). Fuzzy sets. Information and Control, 8(3), 338–353. https://doi.org/10.1016/S0019-9958(65)90241-X

Zhou, L., Miller, J., Vezza, J., Mayster, M., Raffay, M., Justice, Q., Al Tamimi, Z., Hansotte, G., Sunkara, L. D., & Bernat, J. (2024). Additive manufacturing: A comprehensive review. Sensors, 24(9), 2668. https://doi.org/10.3390/s24092668

Received: Jan 1, 2026. Accepted: Aug 4, 2026